INTERNATIONAL CENTRE FOR THEORETICAL PHYSICS

Miramar - Trieste, Italy

SMR.282/14

Second School on ADVANCED TECHNIQUES IN COMPUTATIONAL PHYSICS

18 January - 12 February 1988

COMPUTATIONAL TECHNIQUES IN GEOPHYSICS

by

G. F. Panza

Institute of Geodesy and Geophysics, University of Trieste

International School for Advanced Studies, Trieste

1. Introduction

Earth sciences are concerned with the investigation of the state and the state change of the entire Earth's body, governed by an interplay between various physical and chemical processes and described in a space-time frame. The recent progress, quantitatively and qualitatively remarkable, in the knowledge of the internal properties of our planet can be largely ascribed to the development of computer algorithms tending to the best possible exploitation of available computers. It is also easy to predict that in the near future the possibility given by vector computers to construct highly realistic models will allow the understanding of several physical and chemical processes taking place within the Earth. This in turn will allow to construct dynamical models of the Earth which are essential for predicting its tectonic evolution. A very practical aspect of this procedure may be the possibility of predicting earthquakes, combining the statistical aspects of seismicity with the understanding of seismogenetic processes.

In these lectures I have choosen to describe very briefly some key problems in Geodesy and Seismology whose solution heavily depends upon the availability of highly advanced computer codes which may make the best possible use of the presently available supercomputers.

Geodesy is concerned with the determination of both the shape of the Earth's surface and the Earth's external gravity field. Seismology is concerned with the determination of both elastic and anelastic properties of the Earth interior, which contain also information about density distribution.

According to Newton's law of gravitation, the source of the Earth's gravitational field is the mass distribution within the Earth's surface. According to potential theory, the external gravitational potential of a body can be uniquely determined without the knowledge of any density information if both its shape and the gravitational potential at its surface are known. Unfortunately we neither know the geometry of the Earth's surface with sufficient accuracy, nor we do know the potential at each surface point. Therefore, we have to employ approximation methods and have to use some kind of initial model. Here there are basically two approaches: the **source approach** and the **effect approach**. In the source approach the model is a low-resolution global 3-D density pattern, derived primarily from seismological measurements. In the effect approach the model is a medium resolution global gravity field model, derived from satellite and surface gravity data. Because of the easier access to that information, practically all gravity field approximation methods use the second approach.

Only recently some attempts are being made to use the source approach. The implementation of advanced computer codes will make this approach more and more popular and powerful. Even more, the current interest of seismologists and theoreticians focuses strongly on methods which allow the treatment of laterally heterogeneous media, therefore it will be possible to obtain a starting global 3-D density pattern with a resolution much larger than the one characterizing the models presently available.

2. Models of the Earth's gravity field

According to Newton's law of gravitation the gravitational potential, A, is the integral effect of the mass density distribution with the reciprocal space distance as integral kernel

$$A(P) = G \int_{\tau} l^{-1}(P,Q)\, \varrho(Q)\, dv(Q) \qquad (1)$$

with

P = calculation point,

Q = integration point,

G = gravitational constant,

l = space distance,

ρ = mass density,

v = volume of integration (Earth's body).

It is well known from potential theory that there is an infinite number of mass density distributions possible which generate one and the same potential; therefore ρ cannot be uniquely determined from gravity field data only. However, according to potential theory we can theoretically determine the gravity field from surface gravity field data, measured at the unknown surface of the Earth, directly, by-passing its source, the mass density distribution. This is the meaning of the fundamental integral equation of physical geodesy

$$-2\pi W + \iint_S \left[W \frac{\partial}{\partial n}(l^{-1}) + l^{-1} g_n \right] dS + 2\pi\omega^2(x^2 + y^2) + 2\omega^2 \iiint_v l^{-1}\, dv = 0 \qquad (2)$$

with

S = unknown Earth's surface,

n = outer surface normal,

$\partial/\partial n$ = derivative along surface normal n,

W = A+C = gravity potential,

C = centrifugal potential,

g_n = $-\partial W/\partial n$ = -grad W.n = -g.n,

g = gravity.

If W and g are given on S it is theoretically possible to determine S.

Among all equipotential surfaces there is one distinguished surface which is of considerable concern to Earth sciences: the geoid. It is the surface of constant gravity potential $W = W^\circ$ at mean sea level and coincides with the open ocean surface, considered at rest and not affected by the attraction of celestial bodies. The geoid is the physical-mathematical surface of the Earth and serves as zero level for physical-geodetic height measurements.

About two millenia ago it was realized that the shape of the Earth is approximately a sphere. Two and a half centuries ago that sphere has been replaced by a better approximation, an ellipsoid of revolution. This model is so simple that only four parameters are needed to completely describe both the shape of the ellipsoid and its gravity field

$GM = 3.986005.10^{14}\ m^3\ s^{-2}$ $\qquad J_2 = 1.08263.10^{-3} \sim$ flattening

$a = 6.378137.10^{6}\ m$ $\qquad \omega = 7.292115.10^{-5}\ rad\ s^{-1}$

No model mass density distribution has been used to define

the model gravity field. Therefore, such a model is referred to as "effect model".

More elaborate models represent the Earth's gravity field in terms of a set of spectral coefficients (spherical harmonic coefficients) which are derived from surface and satellite data:

$$W_M(P) = \frac{GM}{r_P}\left\{1 + \sum_{n=2}^{N_M}\sum_{m=0}^{n}\left(\frac{a}{r_P}\right)^n P_{nm}(\cos\theta_P)\cdot \right.$$
$$\left. \cdot\,[C_{nm}\cos(m\lambda_P) + S_{nm}\sin(m\lambda_P)]\right\} + C(P) \qquad (3)$$

with

(r,θ,λ) = spherical coordinates (radius, polar distance, longitude)

$P_{nm}(\cos\theta)$ = fully normalized associated Legendre function

n,m = degree, order

N_M = highest degree of model

W_M = model gravity potential

C_{nm}, S_{nm} = harmonic coefficients.

Routinely Earth models are based on 33000 to 40000 harmonic coefficients, i.e. in (3) N_M = 180 to 200. The most detailed model at present is constructed with N_M = 360 and consists of about 130000 coefficients. These models being

derived from observed satellite and surface gravity field data can be defined effect models, although the harmonic coefficients do bear source information in terms of an integral information about the mass density distribution

$$\begin{Bmatrix} C_{nm} \\ S_{nm} \end{Bmatrix} = \frac{M^{-1}}{2n+1} \int_v \left(\frac{r}{a}\right)^n \bar{P}_{nm}(\cos\theta) \begin{Bmatrix} \cos(m\lambda) \\ \sin(m\lambda) \end{Bmatrix} \varrho(r,\theta,\lambda)\, dv\,. \qquad (4)$$

Equations (3) and (4) clearly demonstrate the relation between source and effect: if a model mass density distribution $\rho(r,\theta,\lambda)$ is available, the corresponding harmonic coefficients of the gravitational potential follow immediately. This concept is at the base of the present strong efforts to develop source Earth models by using seismological information, taking advantage of the availability of extremely powerful computers.

Once a model is constructed it is of key relevance for an improvement of our knowledge to remove the model contributions from the observed gravity field data. This procedure yields data residuals which can be used for the corrections of the parameters defining the initial model. This procedure, is an extremely laborious and computer-time-consuming task. Consider, for example, the representation of the Earth's gravity field model in terms of the harmonic series (3). In this case the computation of the approximate

model means applying for each individual data an operator (which characterizes the data) to all harmonic functions of eq. (3). The Earth Models with about 33000 and 40000 parameters require a tremendous effort, putting a particularly strong emphasis on very well-designed and optimized computer algorithms. This is even more important when routine use will be made of models consisting of 130000 parameters.

If high resolution 3-D source Earth models are used instead of effect models, the computational requirements remain practically the same.

3.1 Wave propagation in layered media

The knowledge of the elastic properties of the Earth's interior is not only relevant for geodetic purposes but it is also very important per se. In spite of the very considerable efforts made by seismologists and theoreticians, it is still missing a satisfactory theory which describes wave propagation in 3-D models of the Earth. If we exclude numerical procedures based on finite differences or finite element methods, extremely time consuming even with the presently available supercomputers, all the existing analytical methods involve significant approximations.

Here I will present the computational aspects of a

method which is free from any approximation in the one dimensional case and which can be quite efficiently extended, introducing approximations of variable entity, to 2-D and 3-D cases by making use of the present availability of supercomputers. The method is commonly known as **Modal summation method.**

We assume that the medium consists of homogeneous layers, separated by first-order discontinuities. If a medium is continuously inhomogeneous (throughout or piecewise), it is replaced by a sufficiently large number of homogeneous layers; in smooth gradient zones it is usually enough to choose roughly half the dominant wavelength as layer thickness, whereas in transition zones with larger velocity gradients the layer thickness should be reduced further. The advantage of the homogeneous-layer approximation is that inside each layer the equation of motion takes a relatively simple form. Its disadvantage is that boundary conditions have to be fulfilled at many interfaces. Analytical methods for inhomogeneous layers (in contrast to numerical, e.g. finite-difference, methods) are not yet developed to a point where they really can compete with the methods for homogeneous layers.

The equation of motion of a homogeneous, isotropic elastic medium is

$$\rho\ddot{u} = (\lambda+2\mu)\,\text{grad div } u - \mu \text{ rot rot } u, \qquad (5)$$

where u is the displacement vector, ρ the density and λ and μ the Lamé parameters. Body forces due to gravity and seismic sources are not included in Eq. (5): it is assumed that gravity has no other effect than to determine, via self-compression, the (constant) values of ρ, λ and μ, and sources of seismic waves are included through their known contributions to u.

In order to simplify the discussion as far as possible, we shall consider solutions of the elastic equations of motion in the form of plane waves rather than attempt to treat the more complex case of waves diverging from a point-source. This does not involve loss of generality in the computation of the dispersion function since the point-source solution may be developed by integration of plane-wave solutions.

Let us consider plane waves of angular frequency p and horizontal phase velocity c propagated in a semi-infinite medium made up of n parallel, homogeneous, isotropic layers. In these lectures, all layers will be assumed to be solid.

The x axis is taken parallel to the layers with the positive sense in the

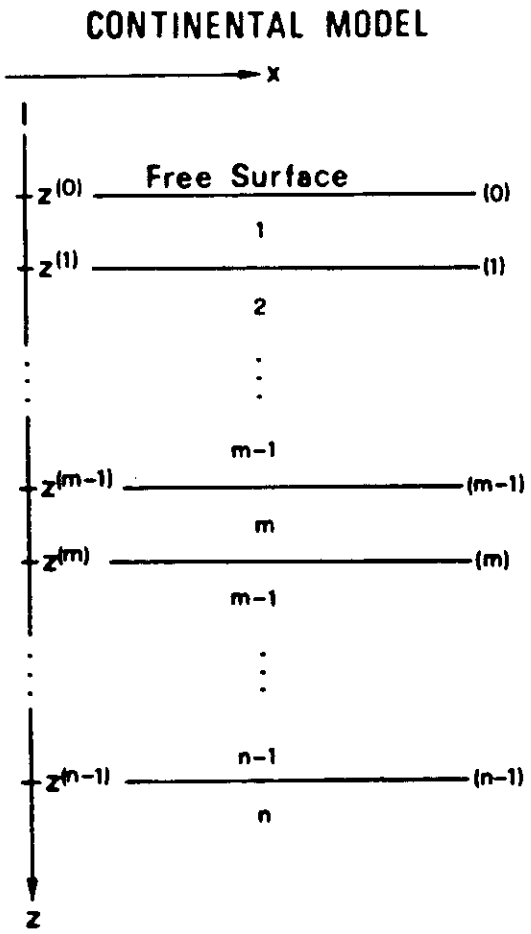

Fig. 1. Direction of axes and numbering of layers and interfaces.

direction of propagation. The positive z axis is taken as directed into the medium. The various layers and interfaces are numbered away from the free surface, as shown in figure 1. We confine our attention to waves of Rayleigh type (P-SV motion), by which we mean that there is no displacement in the y direction and that the amplitude diminishes exponentially in the +z direction in the semi-infinite layer.

For the m-th layer let

ρ_m = density, d_m = thickness, λ_m, μ_m = Lamé elastic constants,

$\alpha_m = \left[(\lambda_m + 2\mu_m)/\rho_m\right]^{\frac{1}{2}}$ = velocity of propagation of dilatational waves

$\beta_m = \left[\mu_m/\rho_m\right]^{\frac{1}{2}}$ = velocity of propagation of rotational waves

$k = p/c = 2\pi/$wave length (horizontal)

$$r_{\alpha m} = \begin{cases} +\left[(c/\alpha_m)^2 - 1\right]^{\frac{1}{2}} & \text{if } c > \alpha_m \\ -i\left[1-(c/\alpha_m)^2\right]^{\frac{1}{2}} & \text{if } c < \alpha_m \end{cases} \qquad \text{if } m < n$$

$$r_{\beta m} = \begin{cases} +\left[(c/\beta_m)^2 - 1\right]^{\frac{1}{2}} & \text{if } c > \beta_m \\ -i\left[1-(c/\beta_m)^2\right]^{\frac{1}{2}} & \text{if } c < \beta_m \end{cases}$$

$$r_{\alpha m} = -i(1 - c^2/\alpha^2_m)^{\frac{1}{2}} \qquad \text{if } m = n$$

$$r_{\beta m} = -i(1 - c^2/\beta^2_m)^{\frac{1}{2}}$$

$\gamma_m = 2(\beta_m/c)^2$

u_m, w_m = displacement components in x and z directions

σ_m = normal stress

τ_m = tangential stress

Then, as is well known, periodic solutions of the elastic equation of motion for the m-th layer may be found by combining dilatational wave solutions,

$$\Delta_m=(\partial u_m/\partial x)+(\partial w_m/\partial z)=$$

$$=\exp[i(pt-kx)][\Delta'_m\exp(-ikr_{\alpha_m}z)+\Delta''_m\exp(ikr_{\alpha_m}z) \tag{6}$$

with rotational wave solutions,

$$\omega_m=(1/2)[(\partial u_m/\partial z)-(\partial w_m/\partial x)]=$$

$$=\exp[i(pt-kx)][\omega'_m\exp(-ikr_{\beta_m}z)+\omega''_m\exp(ikr_{\beta_m}z) \tag{7}$$

where Δ'_m, Δ''_m, ω'_m and ω''_m are constants. With the sign conventions defined above, the term in Δ'_m represents a plane wave whose direction of propagation makes an angle $\cot^{-1} r_{\alpha_m}$ with the +z direction when r_{α_m} is real, and a wave propagated in the +x direction with amplitude diminishing exponentially in the +z direction when r_{α_m} is imaginary. Similarly, the term in Δ''_m represents a plane wave making the same angle with the -z direction when r_{α_m} is real and a wave propagated in the +x direction with amplitude increasing exponentially in the +z direction when r_{α_m} is imaginary. The same remarks apply to the terms in ω'_m and

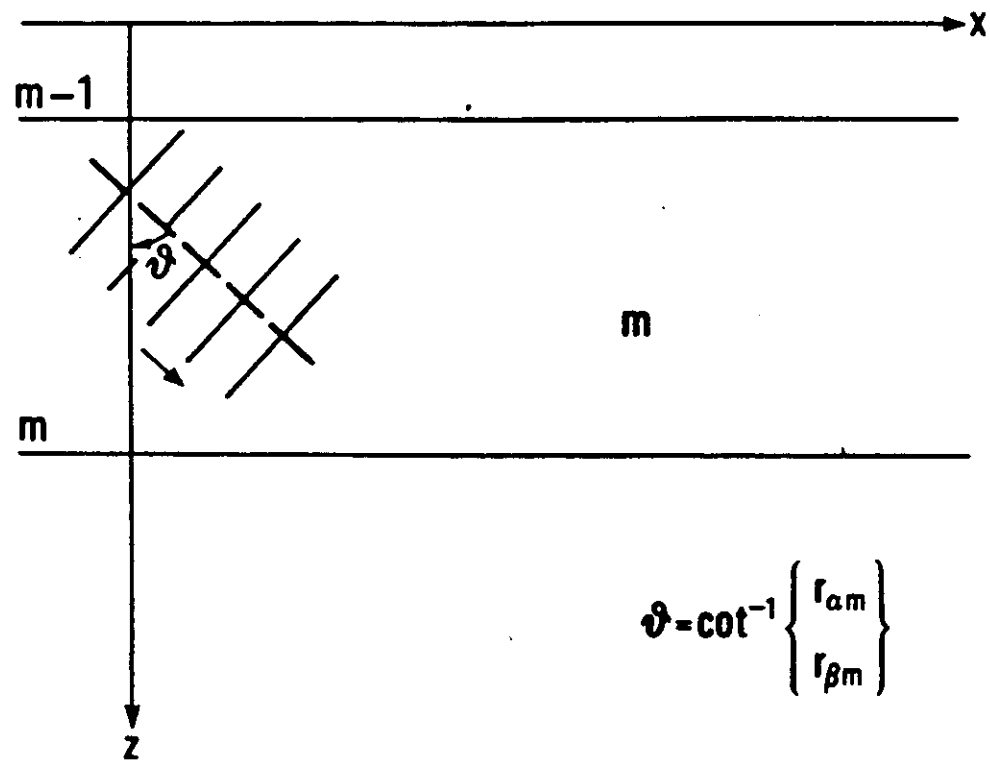

Fig. 2a. Plane waves associated to Δ'_m or ω'_m when $r_{\alpha m}$ (P-wave) or $r_{\beta m}$ (S-wave) are real.

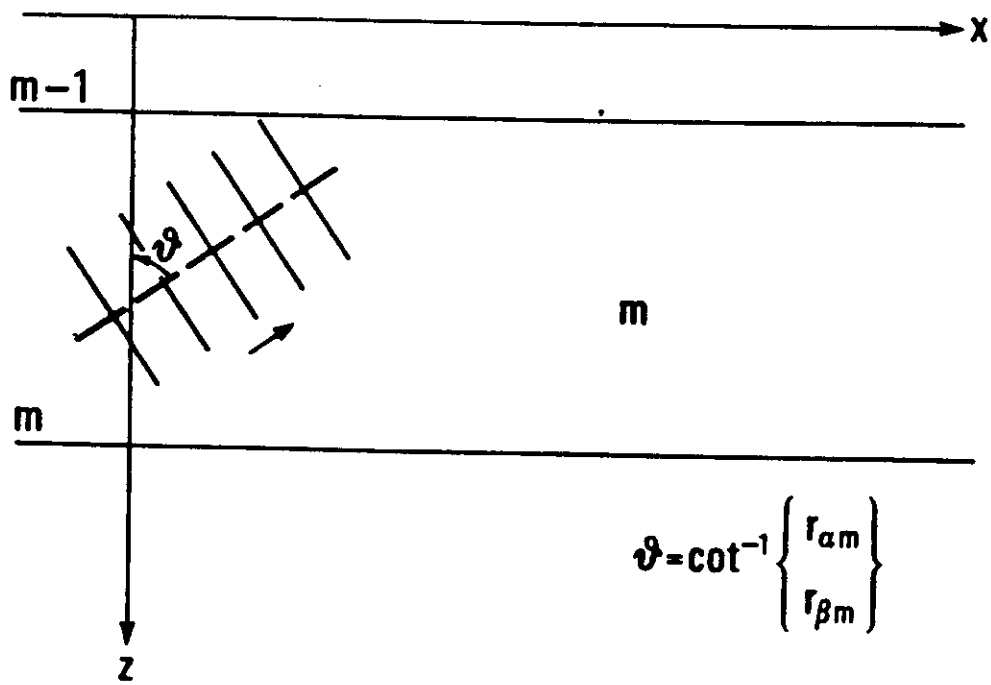

Fig. 2b. Plane waves associated to Δ''_m or ω''_m when r_{α_m} (P-wave) or r_{β_m} (S-wave) are real.

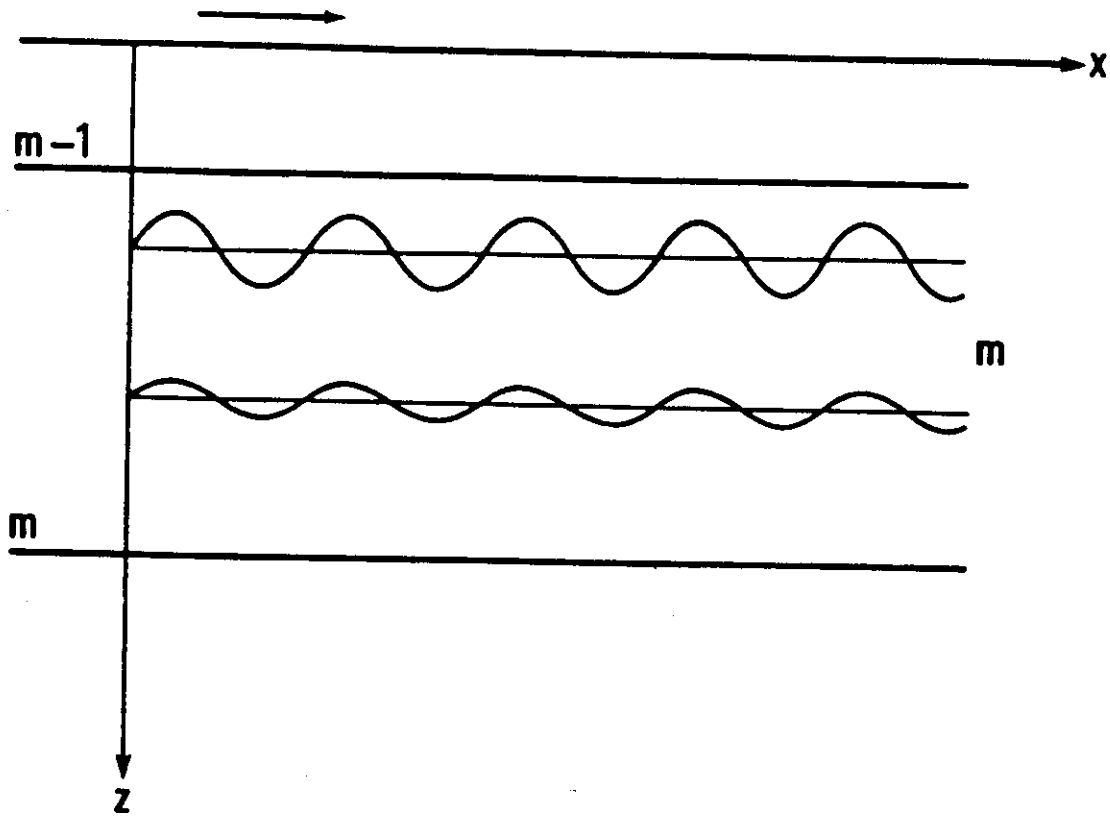

Fig. 2c. Wave propagating in the x direction with amplitude decreasing with increasing depth associated to Δ'_m or ω'_m when r_{α_m} (P-wave) or r_{β_m} (S-wave) are imaginary.

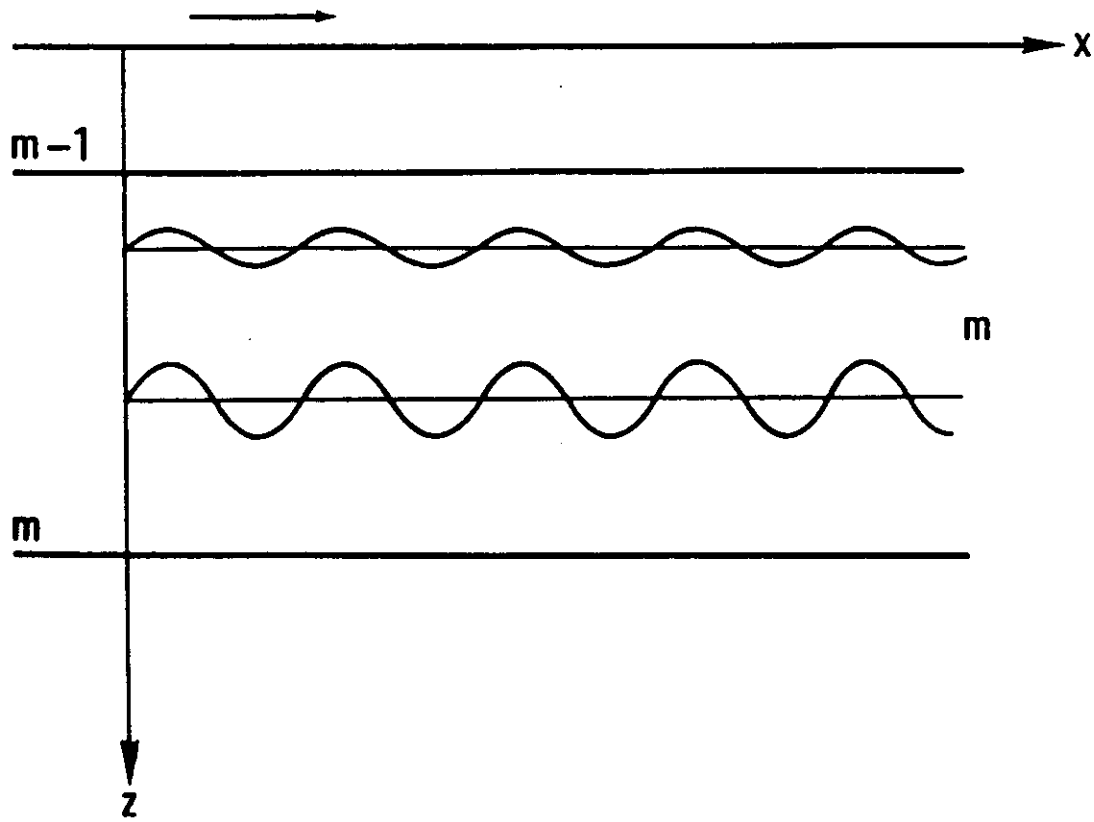

Fig. 2d. Wave propagating in the x direction with amplitude increasing with increasing depth associated to Δ''_m or ω''_m when r_{α_m} (P-wave) or r_{β_m} (S-wave) are imaginary.

ω''_m with r_{β_m} substituted for r_{α_m} (see Fig. 2a, 2b, 2c, 2d).

The displacements and the pertinent stress components corresponding to the dilatation and rotation given by (6) and (7) are,

$$u_m=-(\alpha_m/p)^2(\partial\Delta_m/\partial x)-2(\beta_m/p)^2(\partial\omega_m/\partial z)$$

$$w_m=-(\alpha_m/p)^2(\partial\Delta_m/\partial z)+2(\beta_m/p)^2(\partial\omega_m/\partial x)$$

$$\sigma_m=\rho_m[\alpha^2_m\Delta_m+2\beta^2_m\{(\alpha_m/p)^2(\partial^2\Delta_m/\partial x^2)+ \tag{8}$$

$$+2(\beta_m/p)^2(\partial^2\omega_m/\partial x\partial z)\}]$$

$$\tau_m=2\rho_m\beta^2_m[-(\alpha_m/p)^2(\partial^2\Delta_m/\partial x\partial z)+$$

$$+(\beta_m/p)^2\{(\partial^2\omega_m/\partial x^2)-(\partial^2\omega_m/\partial z^2)\}]$$

The boundary conditions to be met at an interface between two layers require that these four quantities should be continuous. Continuity of the displacements is assured if the corresponding velocity components $\dot{u}_m$ and $\dot{w}_m$ are made continuous and, since c is the same in all layers, we may take the dimensionless quantities $\dot{u}_m/c$ and $\dot{w}_m/c$ to be continuous. Substituting the expressions (6) and (7) in

equations (8) and expressing the exponental functions of ikrz in trigonometric form, we find

$$
\begin{aligned}
u_m &= A_m \cos p_m - i B_m \sin p_m \\
&\quad + r_{\beta_m} C_m \cos q_m - i r_{\beta_m} D_m \sin q_m, \\
w_m &= -i r_{\alpha_m} A_m \sin p_m + r_{\alpha_m} B_m \cos p_m \\
&\quad + i C_m \sin q_m - D_m \cos q_m, \\
\sigma_m &= \rho_m(\gamma_m - 1) A_m \cos p_m - i \rho_m(\gamma_m - 1) \\
&\quad \cdot B_m \sin p_m + \rho_m \gamma_m r_{\beta_m} C_m \cos q_m \\
&\quad - i \rho_m \gamma_m r_{\beta_m} D_m \sin q_m, \\
\tau_m &= i \rho_m \gamma_m r_{\alpha_m} A_m \sin p_m - \rho_m \gamma_m r_{\alpha_m} \\
&\quad \cdot B_m \cos p_m - i \rho_m(\gamma_m - 1) C_m \sin q_m \\
&\quad + \rho_m(\gamma_m - 1) D_m \cos q_m.
\end{aligned}
\tag{9}
$$

where

$$
\begin{aligned}
A_m &= -\alpha_m^2(\Delta'_m + \Delta''_m), & B_m &= -\alpha_m^2(\Delta'_m - \Delta''_m), \\
C_m &= -2\beta_m^2(\omega'_m - \omega''_m), & D_m &= -2\beta_m^2(\omega'_m + \omega''_m), \\
p_m &= k r_{\alpha_m}[z - z^{(m-1)}], & q_m &= k r_{\beta_m}[z - z^{(m-1)}].
\end{aligned}
$$

ρ_m is the density, $z^{(m-1)}$ is the depth of the upper interface of the m-th layer and Δ'_m, Δ''_m, ω'_m, ω''_m are constants appearing in the depth-dependent part of the dilatational and rotational wave solutions:

$$\begin{aligned} &\Delta'_m \exp(-ik r_{\alpha_m} z) + \Delta''_m \exp(ik r_{\alpha_m} z), \\ &\omega'_m \exp(-ik r_{\beta_m} z) + \omega''_m \exp(ik r_{\beta_m} z). \end{aligned} \tag{10}$$

3.2 Fast version of Knopoff's method

For a continental model, the vanishing of the two components of stress at the free surface yields:

$$\begin{aligned} &-\rho_1(\gamma_1 - 1) A_1 - \rho_1 \gamma_1 r_{\beta_1} C_1 = 0, \\ &\rho_1 \gamma_1 r_{\alpha_1} B_1 - \rho_1(\gamma_1 - 1) D_1 = 0. \end{aligned} \tag{11}$$

Thus Knopoff's submatrix $\Lambda^{(0)}$ can be written in the form

$$\Lambda^{(0)} = \begin{bmatrix} -\rho_1(\gamma_1 - 1) & 0 & -\rho_1 \gamma_1 & 0 \\ 0 & \rho_1 \gamma_1 & 0 & -\rho_1(\gamma_1 - 1) \end{bmatrix}. \tag{12}$$

At the m-th interface, the continuity of displacement and stress yields

$$
\begin{aligned}
&A_m \cos P_m - i B_m \sin P_m + r_{\beta_m} C_m \cos Q_m - i r_{\beta_m} D_m \sin Q_m \\
&\quad = A_{m+1} + r_{\beta_{m+1}} C_{m+1}, \\
&-i r_{z_m} A_m \sin P_m + r_{z_m} B_m \cos P_m + i C_m \sin Q_m - D_m \cos Q_m \\
&\quad = r_{z_{m+1}} B_{m+1} - D_{m+1}, \\
&\rho_m(\gamma_m - 1) A_m \cos P_m - i \rho_m(\gamma_m - 1) B_m \sin P_m \\
&\qquad + \rho_m \gamma_m r_{\beta_m} C_m \cos Q_m - i \rho_m \gamma_m r_{\beta_m} D_m \sin Q_m \\
&\quad = \rho_{m+1}(\gamma_{m+1} - 1) A_{m+1} + \rho_{m+1} \gamma_{m+1} r_{\beta_{m+1}} C_{m+1}, \\
&i \rho_m \gamma_m r_{z_m} A_m \sin P_m - \rho_m \gamma_m r_{z_m} B_m \cos P_m \\
&\qquad - i \rho_m(\gamma_m - 1) C_m \sin Q_m + \rho_m(\gamma_m - 1) D_m \cos Q_m \\
&\quad = -\rho_{m+1} \gamma_{m+1} r_{z_{m+1}} B_{m+1} + \rho_{m+1}(\gamma_{m+1} - 1) D_{m+1},
\end{aligned}
\tag{13}
$$

where $P_m = k r_{\alpha_m} d_m$, $Q_m = k r_{\beta_m} d_m$ and d_m is the layer thickness. Thus, Knopoff's 4x8 interface submatrices have the form

$$
\Lambda^{(m)} = \begin{bmatrix}
\cos P_m & -i \sin P_m / r_{z_m} & \cos Q_m & & \\
-i r_{z_m} \sin P_m & \cos P_m & i \sin Q_m / r_{\beta_m} & & \\
\rho_m(\gamma_m - 1) \cos P_m & -i \rho_m(\gamma_m - 1) \sin P_m / r_{z_m} & \rho_m \gamma_m \cos Q_m & & \\
i \rho_m \gamma_m r_{z_m} \sin P_m & -\rho_m \gamma_m \cos P_m & -i \rho_m(\gamma_m - 1) \sin Q_m / r_{\beta_m} & & \\
-i r_{\beta_m} \sin Q_m & -1 & 0 & -1 & 0 \\
-\cos Q_m & 0 & -1 & 0 & 1 \\
-i \rho_m \gamma_m r_{\beta_m} \sin Q_m & -\rho_{m+1}(\gamma_{m+1} - 1) & 0 & -\rho_{m+1} \gamma_{m+1} & 0 \\
\rho_m(\gamma_m - 1) \cos Q_m & 0 & \rho_{m+1} \gamma_{m+1} & 0 & -\rho_{m+1}(\gamma_{m+1} - 1)
\end{bmatrix}
\tag{14}
$$

and, noting that in the half-space $A_n = B_n = -\alpha_n^2 \Delta_n'$

$C_n=D_n=-2\beta^2{}_n\omega'_n$, the submatrix representing the (n-1)th interface has the form

$$\Lambda^{(n-1)}=\begin{bmatrix} \cdots & -1 & -r_{\beta_n} \\ \cdots & -r_{z_n} & 1 \\ \cdots & -\rho_n(\gamma_n-1) & -\rho_n\gamma_n r_{\beta_n} \\ \cdots & \rho_n\gamma_n r_{z_n} & -\rho_n(\gamma_n-1) \end{bmatrix}. \qquad (15)$$

where the first four columns are the same as those of $\Lambda^{(m)}$ with m=n-1. It may be worth observing here that, for each layer, $\Lambda^{(i)}$ (i=1,n) submatrices represent the denominators of Cramer's system solutions when the boundary conditions are applied.

In more compact notation we can write

$$\Delta_R = \begin{vmatrix} \Lambda^{(0)} & & & & \\ & \Lambda^{(1)} & & & \\ & & \ddots & & \\ & & & \Lambda^{(n-2)} & \\ & & & & \Lambda^{(n-1)} \end{vmatrix} \qquad (16)$$

where the non-zero elements only are pictured.

A condition for surface waves to exist is $\Delta_R=0$, which defines the dispersion function for Rayleigh waves

$$F_R(p,c) = \Delta_R = 0 \tag{17}$$

If we limit our attention to the case of solid Earth models, the Rayleigh wave dispersion function, $F_R(p,c)$, has the form

$$F_R(p,c)=T^{(o)}\bar{F}^{(1)}F^{(2)}\bar{F}^{(3)}\ldots \begin{cases} F^{(n-2)}\bar{F}^{(n-1)}T^{(n)}_{solid} & \text{(a)} \\ \bar{F}^{(n-2)}F^{(n-1)}\bar{T}^{(n)}_{solid} & \text{(b)} \end{cases} \tag{18}$$

(a) if n is even,

(b) if n is odd.

which has the symbolic matrix form (1x6)(6x6)...(6x6)(6x1). The elements of these matrices are

$$T^{(0)} = [-\gamma_1(\gamma_1 - 1), 0, (\gamma_1 - 1)^2, \gamma_1^2, \quad 0 \quad , \gamma_1(\gamma_1 - 1)], \tag{19}$$

$$F^{(m)} = \begin{bmatrix} F^{(m)}_{1212} & F^{(m)}_{1213} & F^{(m)}_{1214} & F^{(m)}_{1223} & F^{(m)}_{1224} & F^{(m)}_{1234} \\ F_{1312} & F_{1313} & F_{1314} & F_{1323} & F_{1324} & F_{1334} \\ F_{1412} & F_{1413} & F_{1414} & F_{1423} & F_{1424} & F_{1434} \\ F_{2312} & F_{2313} & F_{2314} & F_{2323} & F_{2324} & F_{2334} \\ F_{2412} & F_{2413} & F_{2414} & F_{2423} & F_{2424} & F_{2434} \\ F_{3412} & F_{3413} & F_{3414} & F_{3423} & F_{3424} & F_{3434} \end{bmatrix}, \qquad (20)$$

$$F^{(m)} = \begin{bmatrix} F^{(m)}_{3434} & -F^{(m)}_{3424} & F^{(m)}_{3423} & F^{(m)}_{3414} & -F^{(m)}_{3413} & F^{(m)}_{3412} \\ -F_{2434} & F_{2424} & -F_{2423} & -F_{2414} & F_{2413} & -F_{2412} \\ F_{2334} & -F_{2324} & F_{2323} & F_{2314} & -F_{2313} & F_{2312} \\ F_{1434} & -F_{1424} & F_{1423} & F_{1414} & -F_{1413} & F_{1412} \\ -F_{1334} & F_{1324} & -F_{1323} & -F_{1314} & F_{1313} & -F_{1312} \\ F_{1234} & -F_{1224} & F_{1223} & F_{1214} & -F_{1213} & F_{1212} \end{bmatrix}, \qquad (21)$$

$$T^{(n)}_{\text{solid}} = \begin{bmatrix} 0 \\ -r_{\alpha n} \\ r_{\alpha n} r_{\beta n} \\ 1 \\ -r_{\beta n} \\ 0 \end{bmatrix} \varepsilon, \qquad T^{(n)}_{\text{solid}} = \begin{bmatrix} 0 \\ r_{\beta n} \\ 1 \\ r_{\alpha n} r_{\beta n} \\ r_{\alpha n} \\ 0 \end{bmatrix} \varepsilon, \qquad (22)$$

The elements $F^{(m)}_{ijkl}$ are obtained from Table I. The quantity $\varepsilon=(-1)^{n-1}\rho^2_1 c^2/\gamma_n r_{\alpha n} r_{\beta n}\rho^2_n\alpha^2_n$ is included in (22) in order that F_R have the same numerical value as the dispersion functions from the Δ-matrix extensions, and the product form of the original Thomson-Haskell formulation.

The basic interface-matrix multiplication in (18) has the symbolic matrix form (1x6)(6x6), where the sixth element of the 1x6 matrix is always the negative of the first element. The symmetry of the 6x6 interface matrices, as indicated below,

$$[U^{(m+1)}, iV^{(m+1)}, W^{(m+1)}, R^{(m+1)}, iS^{(m+1)}, -U^{(m+1)}]$$

$$=[U^{(m)}, iV^{(m)}, W^{(m)}, R^{(m)}, iS^{(m)}, -U^{(m)}]\begin{bmatrix}\delta & 0 & \nu & \upsilon & 0 & \eta\\ i\kappa & \cdot & \cdot & \cdot & \cdot & -i\kappa\\ 0 & \cdot & \cdot & \cdot & \cdot & -0\\ \phi & \cdot & \cdot & \cdot & \cdot & -\phi\\ i\iota & \cdot & \cdot & \cdot & \cdot & -i\iota\\ \eta & 0 & -\nu & -\upsilon & 0 & \delta\end{bmatrix} \quad (23)$$

is the reason that the 1x6 matrix retains this property throughout the formation of the interface-matrix product. The first and last elements of columns 2 and 5 of the 6x6 matrix vanish, which means that fourth-, not sixth-order matrix multiplication is involved in forming the corresponding elements of the 1x6 product matrix. The remaining four elements of the product matrix involve only fifth-order multiplication due to the properties of the

TABLE I

EXPRESSIONS FOR THE QUANTITIES $F_{ij,kl}^{(m)}$

ij \ kl	12	13	14	23	24	34
12	$-\varepsilon_8^{(m)}$	0	$\varepsilon_{13}^{(m)}$	$\varepsilon_6^{(m)}$	0	$\varepsilon_{10}^{(m)}$
13	$-i(\varepsilon_{11}\zeta_9 + \varepsilon_7\zeta_{10})$	$\varepsilon_{15}\zeta_{14}$	$i(\varepsilon_{14}\zeta_9 + \varepsilon_{12}\zeta_{10})$	$i(\varepsilon_9\zeta_9 + \varepsilon_5\zeta_{10})$	$-\varepsilon_{15}\zeta_7$	$i(\varepsilon_{11}\zeta_9 + \varepsilon_7\zeta_{10})$
14	$\varepsilon_{11}\zeta_7 - \varepsilon_7\zeta_{12}$	$i(\varepsilon_{15}\zeta_{10})$	$-\varepsilon_{14}\zeta_7 + \varepsilon_{12}\zeta_{12}$	$-\varepsilon_9\zeta_7 + \varepsilon_5\zeta_{12}$	$i(\varepsilon_{15}\zeta_8)$	$-\varepsilon_{11}\zeta_7 + \varepsilon_7\zeta_{12}$
23	$-\varepsilon_{11}\zeta_{15} + \varepsilon_7\zeta_7$	$i(\varepsilon_{15}\zeta_9)$	$\varepsilon_{14}\zeta_{15} - \varepsilon_{12}\zeta_7$	$\varepsilon_9\zeta_{15} - \varepsilon_5\zeta_7$	$i(\varepsilon_{15}\zeta_{11})$	$\varepsilon_{11}\zeta_{15} - \varepsilon_7\zeta_7$
24	$-i(\varepsilon_{11}\zeta_{11} + \varepsilon_7\zeta_8)$	$-\varepsilon_{15}\zeta_7$	$i(\varepsilon_{14}\zeta_{11} + \varepsilon_{12}\zeta_8)$	$i(\varepsilon_9\zeta_{11} + \varepsilon_5\zeta_8)$	$\varepsilon_{15}\zeta_{13}$	$i(\varepsilon_{11}\zeta_{11} + \varepsilon_7\zeta_8)$
34	ε_{10}	0	$-\varepsilon_{13}$	$-\varepsilon_6$	0	$-\varepsilon_8$

$\varepsilon_0^{(m)} = \rho_{m+1}/\rho_m$

$\varepsilon_1 = \gamma_m - \varepsilon_0\gamma_{m+1}$

$\varepsilon_2 = \varepsilon_1 - 1$

$\varepsilon_3 = \varepsilon_1 + \varepsilon_0$

$\varepsilon_4 = \varepsilon_2 + \varepsilon_0$

$\varepsilon_5 = \varepsilon_1^2$

$\varepsilon_6 = \varepsilon_1\varepsilon_2$

$\varepsilon_7 = \varepsilon_1\varepsilon_3$

$\varepsilon_8^{(m)} = \varepsilon_1^{(m)}\varepsilon_4^{(m)}$

$\varepsilon_9 = \varepsilon_2^2$

$\varepsilon_{10} = \varepsilon_2\varepsilon_3$

$\varepsilon_{11} = \varepsilon_2\varepsilon_4$

$\varepsilon_{12} = \varepsilon_3^2$

$\varepsilon_{13} = \varepsilon_3\varepsilon_4$

$\varepsilon_{14} = \varepsilon_4^2$

$\varepsilon_{15} = -\varepsilon_0$

$\varepsilon_{16} = \varepsilon_8 + \varepsilon_{10}$

$\zeta_1^{(m)} = \cos P_m$

$\zeta_2 = \cos Q_m$

$\zeta_3 = r_{sm}\sin P_m$

$\zeta_4 = \sin P_m/r_{sm}$

$\zeta_5 = r_{gm}\sin Q_m$

$\zeta_6 = \sin Q_m/r_{gm}$

$\zeta_7 = \zeta_1\zeta_2$

$\zeta_8 = \zeta_1\zeta_3$

$\zeta_9^{(m)} = \zeta_1^{(m)}\zeta_6^{(m)}$

$\zeta_{10} = \zeta_2\zeta_3$

$\zeta_{11} = \zeta_2\zeta_4$

$\zeta_{12} = \zeta_3\zeta_5$

$\zeta_{13} = \zeta_4\zeta_5$

$\zeta_{14} = \zeta_3\zeta_6$

$\zeta_{15} = \zeta_4\zeta_6$

first and last elements of the 1x6 matrices. Since the first and last elements of the product matrix are the same except for sign, only one of these two elements needs to be computed. Two fourth-order and three fifth-order multiplications per matrix product is a significant improvement over the original six sixth-order multiplications. If these five product-matrix elements are written out analytically, it is seen that there is still considerable simplification possible by means of simple algebraic factorization. The results of this factorization allow the elements of the product matrix to be written in very simple form. Combining the results of this factorization with the formation of the elements of the new, (m+1)th, 6x6 matrix produces the key portion of the "fast" form of Knopoff's method for Rayleigh wave dispersion computations: For m+1 even,

$$
\begin{aligned}
U^{(m+1)} &= -\varepsilon_{16}^{(m+1)}U^{(m)} + \varepsilon_{11}^{(m+1)}K^{(m+1)} + \varepsilon_{7}^{(m+1)}L^{(m+1)}, \\
V^{(m+1)} &= \varepsilon_{15}^{(m+1)}(\zeta_{14}^{(m+1)}V^{(m)} + \zeta_{10}^{(m+1)}W^{(m)} + \zeta_{9}^{(m+1)}R^{(m)} - \zeta_{7}^{(m+1)}S^{(m)}). \\
W^{(m+1)} &= -\varepsilon_{14}^{(m+1)}K^{(m+1)} - \varepsilon_{12}^{(m+1)}L^{(m+1)} + 2\varepsilon_{13}^{(m+1)}U^{(m)}, \\
R^{(m+1)} &= -\varepsilon_{9}^{(m+1)}K^{(m+1)} - \varepsilon_{5}^{(m+1)}L^{(m+1)} + 2\varepsilon_{6}^{(m+1)}U^{(m)}, \\
S^{(m+1)} &= \varepsilon_{15}^{(m+1)}(-\zeta_{7}^{(m+1)}V^{(m)} + \zeta_{8}^{(m+1)}W^{(m)} + \zeta_{11}^{(m+1)}R^{(m)} + \zeta_{13}^{(m+1)}S^{(m)}),
\end{aligned}
\tag{24}
$$

where

$$K^{(m+1)} = \zeta_9^{(m+1)} V^{(m)} + \zeta_7^{(m+1)} W^{(m)} - \zeta_{15}^{(m+1)} R^{(m)} + \zeta_{11}^{(m+1)} S^{(m)},$$
$$L^{(m+1)} = \zeta_{10}^{(m+1)} V^{(m)} - \zeta_{12}^{(m+1)} W^{(m)} + \zeta_7^{(m+1)} R^{(m)} + \zeta_8^{(m+1)} S^{(m)}, \tag{25}$$

and for m+1 odd,

$$U^{(m+1)} = -\varepsilon_{16}^{(m+1)} U^{(m)} + \varepsilon_{11}^{(m+1)} X^{(m+1)} + \varepsilon_7^{(m+1)} Z^{(m+1)},$$
$$V^{(m+1)} = \varepsilon_{15}^{(m+1)} (\zeta_{13}^{(m+1)} V^{(m)} - \zeta_{11}^{(m+1)} W^{(m)} - \zeta_{13}^{(m+1)} R^{(m)} - \zeta_7^{(m+1)} S^{(m)}),$$
$$W^{(m+1)} = \varepsilon_9^{(m+1)} X^{(m+1)} + \varepsilon_5^{(m+1)} Z^{(m+1)} - 2\varepsilon_6^{(m+4)} U^{(m)}, \tag{26}$$
$$R^{(m+1)} = \varepsilon_{14}^{(m+1)} X^{(m+1)} + \varepsilon_{12}^{(m+1)} Z^{(m+1)} - 2\varepsilon_{13}^{(m+1)} U^{(m)},$$
$$S^{(m+1)} = \varepsilon_{15}^{(m+1)} (-\zeta_7^{(m+1)} V^{(m)} - \zeta_9^{(m+1)} W^{(m)} - \zeta_{10}^{(m+1)} R^{(m)} + \zeta_{14}^{(m+1)} S^{(m)}),$$

where

$$X^{(m+1)} = \zeta_{11}^{(m+1)} V^{(m)} + \zeta_{15}^{(m+1)} W^{(m)} - \zeta_7^{(m+1)} R^{(m)} + \zeta_9^{(m+1)} S^{(m)},$$
$$Z^{(m+1)} = \zeta_8^{(m+1)} V^{(m)} - \zeta_7^{(m+1)} W^{(m)} + \zeta_{12}^{(m+1)} R^{(m)} + \zeta_{10}^{(m+1)} S^{(m)}. \tag{27}$$

The dispersion function is formed by starting with the real quantities

$$
\begin{aligned}
U^{(0)} &= -\gamma_1(\gamma_1 - 1), \\
V^{(0)} &= 0, \\
W^{(0)} &= (\gamma_1 - 1)^2, \\
R^{(0)} &= \gamma_1{}^2, \\
S^{(0)} &= 0
\end{aligned}
\tag{28}
$$

and by repeated applications of Eqs. (24) or (26), until the dispersion function has been carried down to the (n-1)th interface

$$
\begin{aligned}
&[U^{(n-1)}, iV^{(n-1)}, W^{(n-1)}, R^{(n-1)}, iS^{(n-1)}, -U^{(n-1)}] \\
&\qquad = T^{(0)}F^{(1)}F^{(2)}\ldots \begin{cases} F^{(n-1)} & \text{if } n-1 \text{ is even,} \\ F^{(n-1)} & \text{if } n-1 \text{ is odd.} \end{cases}
\end{aligned}
\tag{29}
$$

The complete dispersion function is given by

$$
F_R = [V^{(n-1)}, W^{(n-1)}, R^{(n-1)}, S^{(n-1)}] \begin{cases} \begin{bmatrix} -(1 - c^2/\alpha_n{}^2)^{1/2} \\ -(1 - c^2/\alpha_n{}^2)^{1/2}(1 - c^2/\beta_n{}^2)^{1/2} \\ 1 \\ -(1 - c^2/\beta_n{}^2)^{1/2} \end{bmatrix} \varepsilon & \text{if } n \text{ is even} \\ \begin{bmatrix} (1 - c^2/\beta_n{}^2)^{1/2} \\ 1 \\ -(1 - c^2/\alpha_n{}^2)^{1/2}(1 - c^2/\beta_n{}^2)^{1/2} \\ (1 - c^2/\alpha_n{}^2)^{1/2} \end{bmatrix} \varepsilon & \text{if } n \text{ is odd} \end{cases}
\tag{30}
$$

Since expressions (24)-(28) and (30) involve only real quantities, the use and manipulation of complex numbers is completely avoided in forming the Rayleigh wave dispersion function.

Analogous developments can be made for Earth models containing fluid layers.

The matrix elements for the layers with $c<\beta_m<\alpha_m$, where c is the phase velocity, β_m is the S-wave velocity of the m-th layer and α_m is the P-wave velocity of the m-th layer, contain factors of the form (Schwab, 1970):

$$\begin{matrix}\sinh \\ \cosh\end{matrix} P_m^* \begin{matrix}\sinh \\ \cosh\end{matrix} Q_m^*$$

where

$$P_m^* = -\frac{\omega d_m}{c}\sqrt{1-\frac{c^2}{\alpha_m^2}} = \frac{\omega d_m}{c} r_{\alpha_m}^* \quad \text{real}$$

$$Q_m^* = -\frac{\omega d_m}{c}\sqrt{1-\frac{c^2}{\beta_m^2}} = \frac{\omega d_m}{c} r_{\beta_m}^* \quad \text{real}$$

where d_m is the thickness of the m-th layer and ω is the angular frequency. In the notation used here, the asterisk denotes the imaginary part of an imaginary quantity. For large values of the arguments, the magnitude of these factors is approximated by:

$$\frac{1}{4}\exp\left[\frac{\omega d_m}{c}(r_{\alpha_m}^* + r_{\beta_m}^*)\right].$$

In fact,

$$\sinh P^* = [\exp(P^*) - \exp(-P^*)]/2$$

and

$$\cosh P^* = [\exp(P^*) + \exp(-P^*)]/2$$

which reduces to

$$\sinh P^* \simeq -\exp(-P^*)/2 \qquad \cosh P^* \simeq \exp(-P^*)/2$$

when $P^* \ll 0$; the same for Q^*.

Thus, overflow occurs when the last expression is approximately equal to the maximum value permitted by the computer. Denoting this last quantity as MAX, it is easy to find the limiting values

$$(d_m)_{\text{maximum}} = \frac{c \ln(4 \cdot \text{MAX})}{\omega(r_{\alpha_m}^* + r_{\beta_m}^*)}$$

$$c_{\text{minimum}} = \frac{\omega d_m (r_{\alpha_m}^* + r_{\beta_m}^*)}{\ln(4 \cdot \text{MAX})}$$

$$\omega_{\text{maximum}} = \frac{c \ln(4 \cdot \text{MAX})}{d_m (r_{\alpha_m}^* + r_{\beta_m}^*)}$$

to avoid overflow during the evaluation of the matrix elements for any given layer. If these limits are reached, splitting the thick layers into thinner ones having the same properties does not solve the problem.

A powerful, general solution to the problem of handling homogeneous layers, when they are many wavelengths thick, is the following. When $c<\beta_m<\alpha_m$ and d_m/λ is large, for layer m, it is possible to use the approximation

$$\sinh P_m^* = -\tfrac{1}{2}\exp(k r_{\alpha_m}^* d_m)$$
$$\cosh P_m^* = \tfrac{1}{2}\exp(k r_{\alpha_m}^* d_m)$$

where $k=\omega/c$. The same is valid for $\sinh Q_m^*$ and $\cosh Q_m^*$. It is important to note that these approximated expressions are exact for a finite-precision computer when the magnitudes of P_m^* and Q_m^* increase beyond a certain point. In fact

$$\begin{matrix}\cosh \\ \sinh\end{matrix} x = \tfrac{1}{2}\exp(x) \pm \tfrac{1}{2}\exp(-x).$$

If x increases, reaching the point where

$$\tfrac{1}{2}\exp(-x) = 10^M \tfrac{1}{2}\exp(x),$$

where M is the number of decimal digits carried by the computer, then it is algorithmically exact to use

$$\cosh x = -\sinh x = \tfrac{1}{2}\exp(-x) \qquad x<0.$$

Thus, in Eq. (1) it is possible to factor out the quantity

$$\tfrac{1}{4}\exp[k d_m (r_{\alpha_m}^* + r_{\beta_m}^*)]$$

which is always positive. Since the interest is limited to changes in sign of the dispersion function, this factor can be deleted when treating layer m and consequently there is no more need to deal with exponentials having arguments above a certain level.

The case $\beta_m<c<\alpha_m$ and large d_m/λ can be treated by analogy and it is possible to delete terms like

$$\tfrac{1}{2}\exp(k d_m r_{\alpha_m}^*).$$

The power of this approach has been extensively tested.

Once the phase velocity, c, is obtained for a given angular frequency p, the group velocity, u, is obtained from

$$u = \frac{c}{1-(dc/dp)(p/c)} \tag{31}$$

where standard implicit function theory is applied to the dispersion function, $\mathcal{F}_R$, to obtain

$$\frac{dc}{dp} = -\left(\frac{\partial \mathcal{F}_R}{\partial p}\right)_c \Big/ \left(\frac{\partial \mathcal{F}_R}{\partial c}\right)_p \tag{32}$$

Eq. (32) can be computed from:

$$\left(\frac{\partial \mathcal{F}_R}{\partial p}\right)_c = T^{(0)}\Lambda^{(1)} + \sum_{i=1}^{n-1} \begin{cases} \Gamma^{(i-1)}F^{(i)}\Lambda^{(i+1)} & \text{if } i \text{ is even,} \\ \Gamma^{(i-1)}F^{(i)}\Lambda^{(i+1)} & \text{if } i \text{ is odd,} \end{cases} \tag{33}$$

$$\left(\frac{\partial \mathcal{F}_R}{\partial c}\right)_p = T^{(0)}\bar{\Lambda}^{(1)} + \sum_{i=1}^{n-1}\begin{cases}\Gamma^{(i-1)}F^{(i)}\bar{\Lambda}^{(i+1)} & \text{if } i \text{ is even,}\\ \Gamma^{(i-1)}\bar{F}^{(i)}\Lambda^{(i+1)} & \text{if } i \text{ is odd,}\end{cases}$$
$$+ \begin{cases}\Gamma^{(n-1)}\mathcal{F}^{(n)}_{solid} & \text{if } n \text{ is even,}\\ \Gamma^{(n-1)}\bar{\mathcal{F}}^{(n)}_{solid} & \text{if } n \text{ is odd,}\end{cases} \qquad (34)$$

where

$$\mathcal{F}_R = F_R/\mathcal{E}\,,\quad \mathcal{F}^{(n)}_{solid} = T^{(n)}_{solid}/\mathcal{E}\,,\quad \bar{\mathcal{F}}^{(n)}_{solid} = \bar{T}^{(n)}_{solid}/\mathcal{E}\,,$$

primes indicate the operation $(\partial/\partial p)_c$, dots, the operation $(\partial/\partial c)_p$, and

$$\Gamma^{(i-1)} = \begin{cases} T^{(0)} & i-1 = 0,\\ T^{(0)}F^{(1)}F^{(2)}\cdots F^{(i-2)}F^{(i-1)} & i-1 = 2,4,6,\ldots,n-1,\\ T^{(0)}F^{(1)}F^{(2)}\cdots F^{(i-2)}F^{(i-1)} & i-1 = 1,3,5,\ldots,n-1.\end{cases} \qquad (35)$$

If n is even,

$$\Lambda^{(i+1)} = \begin{cases} F^{(i+1)}F^{(i+2)}F^{(i+3)}\cdots F^{(n-1)}\mathcal{F}^{(n)}_{solid} & i+1 = 2,4,6,\ldots,n-2,\\ \mathcal{F}^{(n)}_{solid} & i+1 = n,\\ \bar{F}^{(i+1)}F^{(i+2)}F^{(i+3)}\cdots F^{(n-1)}\mathcal{F}^{(n)}_{solid} & i+1 = 1,3,5,\ldots,n-1,\end{cases} \qquad (36)$$

and if n is odd,

$$\Lambda^{(i+1)} = F^{(i+1)}F^{(i+2)}F^{(i+3)}\dots F^{(n-1)}\mathcal{F}^{(n)}_{\text{solid}} \qquad i+1 = 2, 4, 6, \dots, n-1,$$

$$\bar{\Lambda}^{(i+1)} = \begin{cases} F^{(i+1)}F^{(i+2)}F^{(i+3)}\dots F^{(n-2)}F^{(n-1)}\mathcal{F}^{(n)}_{\text{solid}} & i+1 = 1, 3, 5, \dots, n-2, \\ \mathcal{F}^{(n)}_{\text{solid}} & i+1 = n. \end{cases} \tag{37}$$

4. Computation of eigenfunctions

The algorithmic details of eigenfunction evaluation by Knopoff's method are rather involved - although in principle only a straightforward application of Cramer's rule is required - whereas the details for the original formulation are quite simple. Thus, the programmer's first hope is once a modified formulation has been successfully employed, to compute an eigenvalue at a frequency where this phase velocity was originally unattainable due to precision loss, and then, to reintroduce this eigenvalue into the original formulation to successfully determine the associated eigenfunctions. Unfortunately this approach does not work. It is therefore necessary to employ a modified version of the original formulation for Rayleigh waves also when computing high-frequency eigenfunctions.

The problem is the evaluation of the eigenfunctions $u(z)$, $w(z)$, $\sigma(z)$, and $\tau(z)$. In the notation of the previous section, this problem reduces to the determination of the constants A_m, B_m, C_m, D_m for the layers above the homogeneous half-space, and the constants A_n and D_n for this deepest structural unit. Our starting point is therefore the linear, homogeneous system of $4n - 2$ equations in $4n - 2$ unknowns

$$\begin{bmatrix} \Lambda^{(0)} & & & \\ & \Lambda^{(1)} & & \\ & & \ddots & \\ & & & \Lambda^{(n-2)} \\ & & & & \Lambda^{(n-1)} \end{bmatrix} \begin{bmatrix} & A_1 \\ r_{\alpha 1} & B_1 \\ r_{\beta 1} & C_1 \\ & D_1 \\ & A_2 \\ r_{\alpha 2} & B_2 \\ r_{\beta 2} & C_2 \\ & D_2 \\ & \vdots \\ & A_{n-1} \\ r_{\alpha n-1} & B_{n-1} \\ r_{\beta n-1} & C_{n-1} \\ & D_{n-1} \\ & A_n \\ & D_n \end{bmatrix} = \begin{bmatrix} 0 \\ \\ \\ \\ \\ \\ \\ \\ \vdots \\ \\ \\ \\ \\ \\ 0 \end{bmatrix}, \tag{38}$$

where the submatrices $\Lambda^{(m)}$ are given by equations (12), (14) and (15). Once the dispersion or eigenvalue problem has been solved by seeking roots of the determinant of the coefficient matrix, we are ready to determine the layer constants. This is done by deleting the last equation of the system and transposing the terms containing D_n to the right-hand side of the equations, thus forming a vector of inhomogeneous terms. If we arbitrarily set D_n to unity, this will force all $r_{\alpha m}B_m$ and D_m to be real, and all A_m and $r_{\beta m}C_m$ to be imaginary. The system now takes the form

$$\begin{bmatrix} & & \\ & & \\ & & \end{bmatrix} \begin{bmatrix} A_1 \\ \vdots \\ r_{\alpha n-1} B_{n-1} \\ r_{\beta n-1} C_{n-1} \\ D_{n-1} \\ A_n \end{bmatrix} = \begin{bmatrix} 0 \\ \vdots \\ 0 \\ r_{\beta n} \\ -1 \\ \rho_n \gamma_n r_{\beta n} \end{bmatrix}, \tag{39}$$

to which we apply Cramer's rule to obtain

$$A_n = \frac{A_n \Delta_n}{\Delta_n}, \tag{40}$$

where the determinants of the numerator and denominator are expressed as matrix products

$$A_n \Delta_n = T^{(0)} F^{(1)} F^{(2)} F^{(3)} \cdots \begin{cases} F^{(n-2)} T_{\Delta\Delta}^{(n-1)} & \text{if } n-1 \text{ is even} \\ F^{(n-2)} T_{\Delta\Delta}^{(n-1)} & \text{if } n-1 \text{ is odd} \end{cases} \tag{41}$$

$$\Delta_n = T^{(0)} F^{(1)} F^{(2)} F^{(3)} \cdots \begin{cases} F^{(n-2)} T_{\Delta}^{(n-1)} & \text{if } n-1 \text{ is even} \\ F^{(n-2)} T_{\Delta}^{(n-1)} & \text{if } n-1 \text{ is odd.} \end{cases} \tag{42}$$

Along with eigenvalues and eigenfunctions, the integral

$$I_1 = \int_0^{\infty} \rho(z)\left\{\left[\frac{\dot{u}^*(z)}{\dot{w}(0)}\right]^2 + \left[\frac{\dot{w}(z)}{\dot{w}(0)}\right]^2\right\} dz \qquad (43)$$

is required in multi-mode synthesis of theoretical seismograms. For a sequence of homogeneous layers, this integral can be written as

$$I_1 = \begin{cases} c^2\{[r_{n-1}B_1] - [D_1]\}^{-2} \sum_{m=1}^{n} I_{(m)} & \text{for a continental structure} \\ c^2\{[r_{n-1}B_1] - [D_1]\}^{-2} \sum_{m=0}^{n} I_{(m)} & \text{for an oceanic structure,} \end{cases} \qquad (44)$$

where

$$I_{(0)} = \int_{z^{(m-1)}}^{z^{(m)}} \rho_0\{[\dot{u}^*(z)]^2 + [\dot{w}(z)]^2\}\, dz \qquad (45)$$

is given by

$$\frac{\rho_0[r_{\alpha 0}B_0]^2}{2\omega c r_{\alpha 0}}\,[\sin P_0 \cos P_0(1 - 1/r_{\alpha 0}^2) + P_0(1 + 1/r_{\alpha 0}^2)]; \tag{46}$$

where

$$I_{(m)} = \int_{z^{(m-1)}}^{z^{(m)}} \rho_m\{[\dot{u}^*(z)]^2 + [\dot{w}(z)]^2\}\,dz,\ 1 \leq m \leq n-1 \tag{47}$$

is given by

$$\begin{aligned}
&\frac{\rho_m}{\omega c}\left\{\frac{1}{2}\left[\zeta_1^{(m)}\zeta_4^{(m)}(([A_m]^*)^2(1 - r_{\alpha m}^2) + [r_{\alpha m}B_m]^2(1 - 1/r_{\alpha m}^2))\right.\right.\\
&\quad + \frac{P_m}{r_{\alpha m}}(([A_m]^*)^2(1 + r_{\alpha m}^2) + [r_{\alpha m}B_m]^2(1 + 1/r_{\alpha m}^2))\\
&\quad + \zeta_2^{(m)}\zeta_6^{(m)}(([r_{\beta m}C_m]^*)^2(1 - 1/r_{\beta m}^2) + [D_m]^2(1 - r_{\beta m}^2))\\
&\quad \left.\left. + \frac{Q_m}{r_{\beta m}}(([r_{\beta m}C_m]^*)^2(1 + 1/r_{\beta m}^2) + [D_m]^2(1 + r_{\beta m}^2))\right]\right.\\
&\quad + \zeta_3^{(m)}\zeta_4^{(m)}([A_m]^*[r_{\alpha m}B_m](1 - 1/r_{\alpha m}^2))\\
&\quad - \zeta_5^{(m)}\zeta_6^{(m)}([r_{\beta m}C_m]^*[D_m](1 - 1/r_{\beta m}^2))\\
&\quad + 2[-\zeta_2^{(m)}\zeta_4^{(m)}[r_{\alpha m}B_m][D_m] + \zeta_1^{(m)}\zeta_6^{(m)}[A_m]^*[r_{\beta m}C_m]^*\\
&\quad + \zeta_1^{(m)}\zeta_2^{(m)}[A_m]^*[D_m]\\
&\quad \left.\left. - [A_m]^*[D_m] - \zeta_4^{(m)}\zeta_6^{(m)}[r_{\alpha m}B_m][r_{\beta m}C_m]^*]\right\};
\end{aligned} \tag{48}$$

and where

$$I_n = \int_{z^{(n-1)}}^{\infty} \rho_n\{[\dot{u}^*(z)]^2 + [\dot{w}(z)]^2\}\,dz \tag{49}$$

is given by

$$\frac{\rho_n}{\omega c}\left\{-\frac{1}{2}\,([A_n]^*)^2(r^*_{\alpha n}+1/r^*_{\alpha n})\right.$$

$$\left.-\frac{1}{2}\,[D_n]^2(r^*_{\beta n}+1/r^*_{\beta n})-2[A_n]^*[D_n]\right\}, \tag{50}$$

with, of course, D_n specified to be unity.

Our tests of the eigenfunction algorithm have been fairly extensive, and have indicated no problems with eigenfunction computations—evaluation of layer constants, and from these, evaluation of displacements and stresses at any depth—up to a frequency of 1,000 Hz; we did not test beyond this point.

Multiple-layer, overflow/underflow control is unchanged from the technique used with eigenvalue—dispersion—computations. This form of solution is possible because identical normalization factors are used in numerator and denominator of the expressions for the layer constants.

However, control of single-layer overflow is more interesting than it is in eigenvalue computations. Our numerical tests with very thick individual layers did not indicate any problems with the computation of layer constants and eigenfunctions; however, these tests did uncover a new loss-of-precision problem with the equation used to determine the energy integral I.

This equation can be used without taking precautions, so long as physically reasonable structures are employed: say, with layer thicknesses that do not exceed by too much, the vertical width of a lobe of the displacement-depth dependences. When this is not true, and a layer becomes several wavelengths thick, precision loss can become noticeable even on graphical representations of I. The reason for this precision loss is easily understood by inspecting the expression for the contribution of a single layer to I

$$\begin{aligned} I_m = {} & \{[K_1(A_m^*)^2 + K_2 A_m^*(r_{\alpha m} B_m)] + [K_3(r_{\alpha m} B_m)^2]\} \\ & + \{[K_4 A_m^*(r_{\beta m} C_m)^* + K_5 A_m^* D_m] + [K_6(r_{\alpha m} B_m)(r_{\beta m} C_m)^* \\ & + K_7(r_{\alpha m} B_m) D_m]\} + \{[K_8((r_{\beta m} C_m)^*)^2 \\ & + K_9(r_{\beta m} C_m)^* D_m] + [K_{10} D_m^2]\}. \end{aligned} \tag{51}$$

Note, from (8), that layer constants A_m and B_m represent compressional-wave contributions, and that layer constants C_m and D_m represent transverse-wave contributions. Thus, returning to (51), the first two terms contain coefficients K_1, K_2, K_3, and are the purely compressional-, or P-wave contributions to the energy integral. The factors of K_1,

K_2, K_3, that are of interest to us here, have the form

$$\begin{matrix}\sin\\ \cos\end{matrix} P_m \begin{matrix}\sin\\ \cos\end{matrix} P_m. \tag{52}$$

The second two terms contain coefficients K_4, K_5, K_6, K_7, and are the coupled-, or P-SV-wave contributions to the integral. The factors of interest in these coefficients are of the form

$$\begin{matrix}\sin\\ \cos\end{matrix} P_m \begin{matrix}\sin\\ \cos\end{matrix} Q_m. \tag{53}$$

The last pair of terms in (51) is the purely transverse-, or SV-wave contribution to the integral and contains coefficients K_8, K_9, K_{10}. The factors that are of interest to us here have the form

$$\begin{matrix}\sin\\ \cos\end{matrix} Q_m \begin{matrix}\sin\\ \cos\end{matrix} Q_m. \tag{54}$$

When $c > \alpha_m > \beta_m$, only sines and cosines of real arguments appear in these three factors, and there is no problem with precision loss. When, for a thick layer, $\alpha_m > c > \beta_m$, these three factors have the forms

$$\begin{matrix}\tfrac{1}{4}\exp(2\,|P_m^*|) & & & \text{for purely } P\text{-wave energy,}\\ \tfrac{1}{2}\exp(|P_m^*|) & \begin{matrix}\sin\\ \cos\end{matrix} & Q_m & \text{for coupled-, } P\text{-}SV\text{-wave energy,}\\ \begin{matrix}\sin\\ \cos\end{matrix} & Q_m & \begin{matrix}\sin\\ \cos\end{matrix} & \text{for purely } SV\text{-wave energy.}\end{matrix} \tag{55}$$

The first two terms in (54) are of opposite sign, with large magnitudes that are nearly equal, the second two terms are of opposite sign, having intermediate magnitudes which are nearly equal, and the last pair of terms are of small magnitude. Schematically, the three pairs of terms have the forms

$$\begin{aligned}&|[N_1 + e] + [-N_1]| +\\ &|[N_2 + d] + [-N_2]| +\\ &|[N_3] + [N_4]|,\end{aligned} \tag{56}$$

where e, d, N_3, and N_4 are of roughly the same order of magnitude. With a finite-precision machine, our computational results show that as $|P_m^*|$ increases and $|N_1|$ becomes larger, e contains fewer and fewer significant figures. Recalling that P is the number of decimal digits carried by the computer, $|N_1|$ finally exceeds e (and $d + N_3 + N_4$) by more than 10^P, the spuriously finite difference $[N_1] - [N_1]$ dominates the true value of I_m, and the calculation therefore has no significance. Thus, just as in the original Thomson-Haskell formulation for Rayleigh-wave

dispersion computations, it is the existence of factors of the form

$$\begin{matrix}\sinh \\ \cosh\end{matrix} P_m^* \begin{matrix}\sinh \\ \cosh\end{matrix} P_m^* \tag{57}$$

that leads to precision problems here. (The details are similar, for precision loss in I, when $\alpha_m > \beta_m > c$.) The simplest solution to this problem is to split a layer into a sequence of thinner layers if the vertical extent of a lobe of the displacement-depth dependences becomes less than the layer thickness; or roughly, if the wavelength of the transverse waves in a layer becomes less than that layer's thickness. Splitting the layers can, of course, be done by simply increasing the number of layers used in the entire program, which is the most desirable solution; since, just when it is required, the density and body-wave velocities in these thinner layers can be varied to obtain a better approximation to the actual structure. However, if it has been decided to use thick layers, it is inefficient to use multiple, juxtaposed, identical layers throughout the whole program, since computation time and cost increase linearly with the number of layers treated by the entire program. It is better to limit the breakup of these layers, only to the I computation; this can be done in such a way as to avoid any significant increase in computation time or cost. The procedure is as follows.

In the initial part of the eigenfunction program it is decided how many times a layer must be divided to avoid precision loss in the evaluation of I. Say that the thick layer, which will be used in its original form right up to the I computation, must be subdivided into g thinner layers (of equal thickness, d_m/g). To avoid all but one set of function calls, which determines execution time in this type of computation, $\sin(P_m/g)$ and $\cos(P_m/g)$ are determined with the usual function calls, and $\sin P_m$ and $\cos P_m$ are then obtained by iterative use of the formulas for the sine and cosine of the sum of two angles. The functions $\sin P_m$ and $\cos P_m$ are then used in the computations up to the point at which I is to be computed. Of course, Q_m is treated in the same way. Then, for the computation of I, layer m is broken into g sublayers, each of which is characterized by the functions

$$\begin{aligned}
Z_1^{(m)} &= \cos(P_m/g) \\
Z_2^{(m)} &= \cos(Q_m/g) \\
Z_3^{(m)} &= r_{\alpha m}\sin(P_m/g) \\
Z_4^{(m)} &= (1/r_{\alpha m})\sin(P_m/g) \\
Z_5^{(m)} &= r_{\beta m}\sin(Q_m/g) \\
Z_6^{(m)} &= (1/r_{\beta m})\sin(Q_m/g).
\end{aligned} \tag{58}$$

Since these quantities have already been computed and saved, no extra expense is incurred in their use. The layer constants which have already been computed for layer m—for the original, thick layer—are also those of the uppermost of the g sublayers: $A^*_{m,1}$, $r_{\alpha m}B_{m,1}$, $(r_{\beta m}C_{m,1})^*$, $D_{m,1}$. With these constants, and the functions $Z_i^{(m)}$ replacing $\zeta_i^{(m)}$, the usual formula for I can be used for the accurate evaluation of this first sublayer's contribution to the integral. The layer constants for the next layer down are

$$\begin{aligned}
(A^*_{m,i+1}) &= Z_1^{(m)}(A^*_{m,i}) - Z_4^{(m)}(r_{\alpha m}B_{m,i}) \\
(r_{\alpha m}B_{m,i+1}) &= Z_3^{(m)}(A^*_{m,i}) + Z_1^{(m)}(r_{\alpha m}B_{m,i}) \\
(r_{\beta m}C_{m,i+1})^* &= Z_2^{(m)}(r_{\beta m}C_{m,i})^* - Z_5^{(m)}(D_{m,i}) \\
(D_{m,i+1}) &= Z_6^{(m)}(r_{\beta m}C_{m,i})^* + Z_2^{(m)}(D_{m,i}).
\end{aligned} \tag{59}$$

These layer constants are also used with the functions $Z_i^{(m)}$, to obtain the second sublayer's contribution to I. This procedure is repeated until the contributions of all g sublayers have been obtained.

5. Mode follower and structure minimization

Since all the problems connected with the loss-of-precision at high frequencies have been solved , the summation of higher modes of surface waves can be used for the generation of "complete" synthetic seismograms also at high frequencies.

The key point in the use of multimode summation is an efficient computation of phase velocity for the different modes at sufficiently small frequency intervals, Δf, and with sufficient precision. To be efficient it is not advisable to determine, at each frequency and for each mode, the zeros of the dispersion function using the standard root-bracketing and root-refining procedure.

This procedure must be used only when strictly necessary, as for instance at the beginning of each mode. For all other points, i, of each mode the phase velocity can be estimated by cubic extrapolation, using the values of the phase slowness s=1/c and df/ds already determined at frequencies f_{i-2} and f_{i-1}. However the

precision which can be reached in this way is not satisfactory, thus the phase velocity value must be refined. This can be done by an iterative cubic fit in the F-c plane. In our experience, such a procedure has given always highly accurate determinations of the phase velocity and allows a considerable time saving compared with the standard root-bracketing root-refining procedure.

Once the problem of an efficient determination of phase velocities is solved, two other main problems must be solved at each frequency:

a) to correctly follow a mode;

b) to determine the minimum number of layers to be used.

The problem of correctly following a mode arises in the high frequency domain ($f > 0.1$ Hz) where several higher modes are very close to each other. The determination of the minimum number of layers to be used - structure minimization - is critical in order to reach a high precision in phase velocity determination spending the minimum possible computer time.

In order to ensure a high efficiency in the computation of synthetic seismograms, it is necessary to compute the basic ingredients in the frequency domain - phase velocity, phase attenuation, group velocity, energy integral and ellipticity - at constant frequency intervals. To reach a maximum frequency of 10 Hz a satisfactory step

turned out to be 0.05 Hz. To determine the total number of modes present in the frequency interval considered we fix c_o=0.98 β_n, where β_n is the S-wave velocity in the half-space, and we increment f, using the Schwab and Knopoff (1972) algorithm to find the values of f corresponding to zeros of the dispersion function $F(f, c_o)$. Obviously, starting from f=0, the first zero in $F(f, c_o)$ corresponds to the fundamental mode, the second to the first higher mode and so on. The values of f for which $F(f, c_o)=0$ are used as starting frequencies (the lowest frequencies) for the computation of the different modes. Once the starting frequency for each mode is defined, it is possible to compute, beginning from the fundamental mode, all dispersion relations. This is accomplished by keeping f fixed and varying c, the procedure being applied at all the equally spaced frequency points of the chosen frequency interval.

5.1 The mode follower

The basic idea is to define an efficient method to follow a given mode M in the phase velocity-frequency space, distinguishing it from the neighbouring modes M-1 and M+1, a problem which is most severe near the osculation points, as, for instance, those characterizing the transition from crustal waves to channel waves. For frequencies as high as 1 Hz the fundamental mode is in

general well separated from the remaining modes, while for higher frequencies this is no longer true. Thus for the construction of synthetic signals containing high-frequency the mode follower must be applied to all modes, including the fundamental. On the basis of our experience up to now, there are no other modes present in the proximity of the near osculations between the fundamental and the first higher mode. To follow the fundamental mode it is therefore sufficient to use the following properties of $\partial F/\partial c$:

a) for a given mode M, the sign of $\partial F/\partial c$ is constant with frequency;

b) going from a mode to the next $\partial F/\partial c$ changes sign with regularity.

In other words, once the sign of $\partial F/\partial c$ is computed at the initial frequency of the fundamental mode, in all subsequent points the simple check of this sign makes it possible to follow the mode correctly. In fact, with increasing frequency, as long as the sign of $\partial F/\partial c$ does not change, the obtained zero of F(f, c) belongs to the fundamental mode. If the sign of $\partial F/\partial c$ changes, the zero of F(f, c) does not belong to the fundamental mode and the search of the zero restarts from a lower value of c. In such a way it is possible to compute all the dispersion curve for the fundamental mode quite rapidly.

For the higher modes the above algorithm is not

sufficient because they are generally much closer to each-other. However the construction of an efficient mode follower is still possible.

For a given higher mode, even if computations are made for structures containing very strong low-velocity layers, the phase velocity decreases with increasing frequency. Thus for each higher mode, M, the possible value of the phase velocity, at a given frequency f, lies in the range (c_1, c_2), where c_1 is the phase velocity of the mode M-1 at the frequency f and c_2 is the phase velocity of the mode M at the frequency $f-\Delta f$. If the computations are carried to a maximum frequency of 1 Hz we suggest a frequency step $\Delta f=0.005$ Hz, while if the maximum frequency is 10 Hz then $\Delta f=0.05$. This condition, combined with the property of the sign of $\partial F/\partial c$ recognizes an eventual jump from mode M to modes M+(2n+1) (n=0,1,...). If in the domain (c_1, c_2) and $(f-\Delta f, f)$ 2m+1 (m=1,2,...) modes are contained, the procedure just outlined is not sufficient to follow the mode. On the basis of our experience we can state that this happens very seldom; thus we have not bothered to derive a very efficient algorithm to solve this problem. Our mode follower recognizes this mode jump only when the computation of modes M+1 and M+2 is completed. At this point the computation can be restarted from the mode M at the

frequency f using as the initial phase velocity a value just slightly greater than that of the mode M-1 at the same frequency.

Even if up to now we have carried out computations for a limited sample of continental and oceanic structural models , we can state that this version of the mode follower is totally satisfactory to compute with high efficiency all the frequency domain ingredients of synthetic seismograms.

As we have seen, body waves are dispersed in anelastic media. The frequency dependence of body waves requires the introduction of a small but essential variation in the mode follower.

In the perfectly elastic case, for each higher mode, M, the possible value of the phase velocity, at a given

frequency, lies in the range (c_1, c_2). When body wave dispersion is present, the upper limit c_2 has to be redifined. The phase velocity of body waves, in fact, increases with increasing frequency and this may cause an increase of the phase velocity of higher modes with frequency. This effect is evident in those parts of the mode curves which are almost undispersed in the perfectly elastic case. One has therefore to estimate the increase in phase velocity of a given mode at a given frequency f, with respect to the frequency f-Δf, due to the dispersion of body waves.

Let us denote by Δc_2 the maximum possible increment of c_2.

It is convenient to express the difference Δc in the phase velocity between the frequencies f-Δf and f, due to the effect of the body wave dispersion, by

$$\Delta c = \frac{c(f)}{1+x \ln \frac{f_0}{f-\Delta f}} \cdot \frac{x \ln \frac{f}{f-\Delta f}}{1+x \ln \frac{f_0}{f}} \qquad (60)$$

with

$$x = \frac{2}{\pi} c(f) C_2(f)$$

The use of (60) is not straightforward, since the value of

Δc depends upon $c(f)$ and $C_2(f)$, quantities which are obviously unknown at this stage of the computation.

In order to estimate Δc one can substitute to $c(f)$ and $C_2(f)$ a weighted average of the S-wave velocities, B_1, and the S-wave phase attenuations, B_2. As weights we use the eigenfunctions at the frequency $f-\Delta f$, in particular the sum of the squared displacements. Therefore

$$\Delta c_2 = \frac{\bar{B}_1(f-\Delta f)}{1-\bar{x}\ \text{ln}\ \frac{f_o}{f-\Delta f}} \cdot \frac{\bar{x}\ \text{ln}\ \frac{f}{f-\Delta f}}{1+\bar{x}\ \text{ln}\ \frac{f_o}{f}} \qquad (61.)$$

with

$$\bar{x} = \frac{2}{\pi}\ \bar{B}_1(f-\Delta f)\ \bar{B}_2(f-\Delta f)$$

It has been found with extensive numerical testing that the above relations yield a very satisfactory definition of the upper limit c_2. In the case the wave at the frequency $f-\Delta f$ penetrates to a much smaller depth than that at the frequency f, as for instance in the channel wave - crustal wave sequence, the weighted averages B_1 and B_2 are computed at the last frequency $f-N\Delta f$, where the wave reaches about the same penetration depth as that at the frequency f. The main advantage of the above modification consists in keeping the general scheme of the perfectly elastic mode-follower the same.

Due to body wave dispersion, care must also be taken in computing group velocities using implicit function theory (Eq. 31-32). When computing $\left(\frac{\partial \mathcal{F}_n}{\partial p}\right)_c$ one has to remember that body wave velocities are functions of frequency. In this case equation (33) contains terms associated with the derivative with respect to the angular frequency, p, of the compressional and shear wave velocities.

The effects of body wave dispersion are not very relevant in practice, however we want to stress that the introduction of body waves dispersion in anelastic media is a physical necessity.

5.2 Structure minimization

The structure minimization is a critical point regarding the efficiency and the accuracy of the computation of eigenvalues, eigenfunctions and related quantities. In order to save computer time, it is necessary to determine for each frequency, the minimum amount of structure to be used in the computation, while retaining very high accuracy. In general for a structure made by n layers this can be done by computing the quantity

$$E_m = \bar{\rho}_m \left[\left(\frac{u_m^*}{w_0} \right)^2 + \left(\frac{w_m}{w_0} \right)^2 \right] \qquad m=1,\ldots n-1 \qquad (62)$$

where

$$\bar{\rho}_m = \frac{\rho_{m-1} + \rho_m}{2} \qquad \text{if} \quad m \geq 2$$

and ρ_{m-1} and ρ_m are the densities in layers m-1 and m, if m=1 $\bar{\rho}_1=\rho_1$.

Since we have chosen for each mode to start from the lowest frequencies consistent with a value of $c=0.98\ \beta_n$, the amount of structure to be used at the beginning of each mode coincides with the total number, n, of layers in the structural model. Once the phase velocity is determined, E_m can easily be computed and starting from m=n-1 it is easy to locate its deepest minimum value.

At this stage all the layers below the interface, j, corresponding to the deepest minimum value of E_m can be discarded and the parameters of the j+1 layer are used to define the half-space. With the minimized structure it is now possible to compute with the necessary accuracy, more than 8 figures, the final value of the phase velocity. In general, repeating this procedure for each frequency and for each mode gives very satisfactory results.

Particular care must be placed in the structure minimization when low velocity layers are present in the structural model. Let us consider here the case of only one low velocity channel, the extension to many velocity inversions being quite obvious. For the waves propagating essentially in the low velocity channel, the necessary accuracy is ensured by simply placing the terminating half-space just below the zone of velocity inversion. For

the waves propagating above the low velocity channel, i.e. for the waves with a phase velocity less than the minimum S-wave velocity in the channel, only the structure above the deepest minimum of E_m located above the channel needs to be retained.

The situation is completely different when dealing with waves propagating with a phase velocity larger than the minimum S-wave velocity in the channel, i.e. for waves mainly propagating above the low velocity channel but sampling also deeper. For these waves it is generally necessary to keep at least all the channel, assigning the properties of the layer immediately below it to the half-space. It must be observed that in many cases the penetration in the low velocity channel is so small, that the structure minimization can be performed, without loosing in precision, by removing the whole channel, with evident time saving. The identification of the waves for which the above reduction is possible can be made by evaluating E_m, starting at m=0. If in some of the layers just above the low velocity layer $E_j \leq 10^{-4} E_o$, then the structure can be terminated at the j-th interface, using as half-space characteristics those of the j-th layer. From the description given above it is clear that the initial amount of structure used for the computation at a given frequency, f, is determined by the result of the structure minimization

at the frequency f-Δf. This is obviously not valid if at the frequency f-Δf there was a wave sampling the channel very weakly ($E_j < 10^{-4} E_0$). In these cases the amount of structure initially used at the frequency, f, contains always the low velocity layer.

References

Aki, K. and Richards, P. G. (1980). "Quantitative Seismology". Freeman and Co., San Francisco.

Ben-Menahem, A. and Sing, S. J. (1981). "Seismic Waves and Sources". Springer, New York.

Colombo, O. L. (1981). Numerical methods for harmonic analysis on the sphere. Report No. 310, Department of Geodetic Science and Surveying. Columbus, Ohio: The Ohio State University.

Dziewonski, A. M. (1984). Mapping the lower mantle: Determination of lateral heterogeneity in P velocity up to degree and order 6. **J. Geophys. Res.**, 89, 5929-5952.

Panza, G. F. (1985). Synthetic seismograms: the Rayleigh waves modal summation. **J. Geophys.**, 58, 125-145.

Panza, G. F. and Suhadolc, P. (1987). Complete strong motion synthetics. **In**: "Seismic Strong Motion Synthetics" (B. A. Bolt, ed.), Computational Techniques 4, 153-204, Academic Press, Orlando.

Rapp, R. H. (1981). The earth gravity field to degree and order 180 using seaset altimeter data, terrestrial gravity data, and other data. Report No. 322, Department of Geodetic Science and Surveying. Columbus, Ohio: The Ohio State University.

Rizos, C. (1979). An efficient computer technique for the evaluation of geopotential from spherical harmonic models. **Anst. J. Geodesy, Photogrammetry and Surveying**, 31, 161-169.

Schwab, F. and Knopoff, L. (1972). Fast surface wave and free mode computations. **In**: "Methods in Computational Physics" (B. A. Bolt, ed.), 11, 87-180. Academic Press, New York.

Tscherning, C. C., Rapp, R. H. and Goad, C. (1983). A comparison of methods for computing gravimetric quantities from high-degree spherical harmonic expansions. **Manuscripta Geodaetica**, 8, 249-272.